PCCP

Accepted Manuscript

ROYAL SOCIETY OF CHEMISTRY

www.rsc.org/pccp

One sentence of 20 words, plus an 8x4 cm image, see TOC.pptx for high resolution image of the TOC

PSD/PCA analysis of MED data allowed enhancing chemical selectivity in X-ray Powder Diffraction and obtaining Xe substructure into MFI zeolite

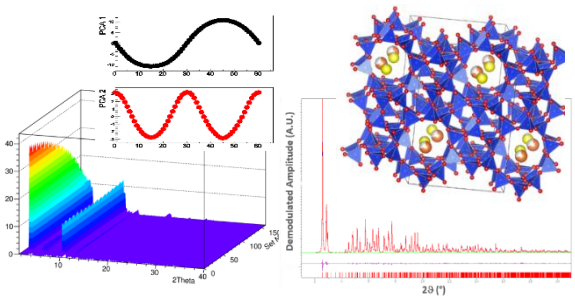

Cite this: DOI: 10.1039/c0xx00000x

www.rsc.org/xxxxxx

ARTICLE TYPE

Chemical selectivity in structure determination by time dependent analysis of in situ XRPD data: a clear view of Xe thermal behavior inside a MFI zeolite

Luca Palin,[a,b] Rocco Caliandro,[c] Davide Viterbo,[a] Marco Milanesio[a,*]

Received (in XXX, XXX) Xth XXXXXXXXX 20XX, Accepted Xth XXXXXXXXX 20XX
DOI: 10.1039/b000000x

X-ray diffraction methods in general provide a representation of the average structure, thus allowing only limited chemical selectivity. As recently shown [Chernyshov, D., et al., Acta Cryst. A, 2011, A67, 327], some structural information on a subset of atoms can be obtained by modulation enhanced diffraction (MED), thus proposing a new tool that is able to enhance selectivity in diffraction. MED uses a periodic stimulus supplied *in situ* on a crystal, while diffraction data are collected continuously during one or more stimulation periods. Such large data sets can then be treated by different methods. Here we present and compare Phase Sensitive Detection (PSD) and Principal Component Analysis (PCA) for in situ X-ray powder diffraction (XRPD) data treatment. The application of PCA to MED data is described for the first time in the present paper. Simulated and experimental MED powder data were produced by using an MFI zeolite as static spectator, in which Xe, acting as active species, is adsorbed and desorbed in a periodic manner. MED allowed obtaining, by demodulating first simulated and then experimental data, the powder diffraction pattern of the responding scattering density, and selectively extracting crystallographic information on Xe by solving the crystal structure of the active species independently of the static zeolite framework. The "real world" experiments indicated that the PSD-MED approach has some limitations related to the degree of fulfilment of some theoretical assumptions. When applied to in situ XRPD data, PCA, despite based on blind statistical analysis, gave results similar to those obtained by PSD (based on Fourier analysis) for simulated data. Moreover, PCA is complementary to PSD, thanks to its capability of gathering information on the Xe substructure even in the presence of a non-periodic stimulus, i.e. using for instance the most simple stimulus shape as a single temperature ramp. In particular PC1 resulted able to perfectly reproduce the corresponding 1Ω signal from a traditional PSD analysis. Moreover PCA can be applied directly to raw non periodic XRPD data, opening the possibility of using it during an "*in situ*" experiment. PCA can thus be envisaged as a very useful fast and efficient tool to improve data collection strategy and to maximize data quality and their information content. To date however PSD remains superior for substructure solution from analysis of 2Ω demodulated data.

1. Introduction

X-ray diffraction (XRD), after almost 100 years of development, has become a very successful technique for the structural characterization of condensed matter. XRD was applied successfully also to complex problems in catalysis, in particular concerning extra-framework species location in microporous materials.[1-5] There are, however, few fundamental limitations of this technique. One of these is represented by its limited chemical selectivity. In fact, XRD does not allow separating contributions from different atomic subsets. It is possible to obtain limited element selectivity by exploiting resonant scattering, but applications are limited to heavy atoms: Z > 15 in principle, but practically Z > 25, in most cases in sufficiently high concentration.[6] In protein crystallography the problem has been addressed by using diffraction data sets from different heavy-atom derivatives, in the case of isomorphous replacement technique,[7] or from measurements at different wavelengths, in the case of anomalous dispersion technique.[8] Proper phasing algorithms have been developed to find at first the substructure formed by the heavy atoms or anomalously scattering atoms respectively, and then to locate the whole protein.[9-11] A further limitation is represented by the difficulty to achieve time-resolved information from the crystal system. Time-resolved experiments have been attempted by using different techniques, such as Laue diffraction and trapped intermediate diffraction studies for protein crystals[12] or by pump and probe experiments.[13] Finally the recently developed XFEL facilities, where the X-ray flux is modulated by definition[14] and the samples is continually refreshed in a periodic fashion, implies the development of novel experimental techniques and data analysis methods, where MED might give an important contribution. In this

respect, the possibility of enhancing the sensitivity and the signal to noise ratio in diffraction experiments aiming at following the evolution of the system in response to an external stimulus, is of paramount importance, especially when applied to complex systems such as macromolecules.[15]

A recent paper[16] proposed a new method, called modulation enhanced diffraction (MED), which is able to overcome the selectivity limitations of diffraction. The method is based on concepts used in Modulation Excitation Spectroscopy (MES), to obtain information on active species diluted into an inactive spectator matrix and/or buried in noise.[17,18] Modulation excitation techniques were successfully exploited in X-ray adsorption spectroscopy techniques.[19,20,21] To extend the approach to XRD and carry out a MED experiment, a periodic stimulus is applied *in situ* on a single crystal or on a powder sample, and diffraction data are treated by a mathematical procedure called "phase sensitive detection (PSD)".[17] The feasibility of modulating the electron density of a sample during an X-ray diffraction experiment was already demonstrated, but the nature and extent of the obtainable information was not explored.[22] One of the implications of the MED theory[16] is that PSD applied to crystallography allows, in principle, filtering only the signal of the sample components responding to the stimulus and thus obtaining the experimental diffraction pattern of the active subset of atoms, while the diffraction signal of the inactive spectator electron density is completely removed. MED theory was at first applied to the special case of structure factor modulation, where the "stimulus" is the varying energy of the incident X-ray beam[23] and to structure solution by Patterson methods.[24] In these cases the collected data were treated with a "single-crystal like" approach, because MED technique was applied to intensities extracted by Le Bail or Pawley methods. Very recently Ferri et al.,[25-28] applied PSD to XRPD and XAS data to unravel the kinetics of solid state reactions, i.e. they treated the "the inverse problem" as defined by Chernyshov et al.[16] In this paper, a mathematical expression for MED applied to X-ray powder data directly (detailed in ESI file, §1), without intensity extraction, is presented. The main implications of this theory were then verified by means of simulated and real experiments for the solution of the "direct problem",[16] i.e. the structural characterization of the responding substructure of a sample. We demonstrated that the demodulated pattern can be treated as a normal XRPD pattern by using standard crystallographic software to obtain directly the structural information on a subset of atoms by an in situ experiment. The demodulation was carried out by two different methods. At first data were treated by PSD followed by Fourier analysis of MED data, as in ref. 23 and 24, but directly on XRPD data, without extracting the integrated Bragg intensities. Then demodulation was carried out by a novel and alternative approach, based on principal component analysis (PCA). PCA was recently applied to energy dispersive in situ XRPD data,[29] but the meaning of PC1 and PC2 was not interpreted in term of MED theory, that at that time (2010) was not yet reported in the literature. Indeed authors already realized the effectiveness and easiness of this approach. The two analysis methods (PSD and PCA) were compared from the view point of performance and easiness of use. As test case, the Xe adsorption/desorption process on/from a Ga-containing MFI zeolite powder sample was induced by pressure or temperature stimulus. This experiment was selected as a "proof of principle" test-case because of the possibility of modulating only one (atom occupancy) among many possible degrees of freedom of the crystal structure. In fact the target is realizing the case described in §6.1 of ref. 16, concerning the stimulus effect on the occupancy of the active atoms. The Xe-MFI system is chosen to serve as an interesting example of an active-spectator interaction, which cannot be rationalized without structural information about the location of Xe inside zeolite channels. To our knowledge, only XAS and computational studies on Xe inside MFI are available,[30] while XRD investigations are not yet reported. Very recently adsorption/desorption Xe in MOF was studied with the aim of reducing Xe purification costs.[31] Information on Xe location and thermal-induced desorption into a zeolite can be useful to improve industrial extraction of Xe[32] and for new hints on the "missing Xe" problem (i.e. the experimentally observed Xe in the environment is smaller than the expected Xe amount as detailed in ref. 33. During the Xe sorption process the zeolite framework is mostly unchanged and acted as spectator, while the periodically adsorbed and desorbed Xe atoms acted as active species, changing their occupancies within the channels linearly with external stimulus, as required for MED theory to be applied for the analysis.[16] As a first result, we prove that, when a system is perturbed by a periodic external stimulus, the structural response of the crystalline materials is also periodic and can be exploited to enhance chemical selectivity in XRD. Second, we present experimental information on the location of Xe atoms and on the thermal behavior of adsorption into MFI, obtained using MED. Finally, potentialities and limitation of PSD and PCA demodulation methods for data analysis are discussed.

1.1 Chemical selectivity in X-ray diffraction: the state of the art and implications of MED

In general, X-ray diffraction suffers from the well-known "crystallographic phase problem" due to the fact that the analytical relationships between the measured diffracted intensities and the electron density (or the atomic positions) in the crystal structure are far from being linear and analytically resoluble. The goal of all structure solution methods is retrieving such "crystallographic phases" to be used in calculating an electron density map to find the atomic positions in a unit cell. Several methods have been developed and are classified as (i) *direct methods* working in reciprocal space, (ii) *real space methods* working in the direct space, and (iii) *hybrid* or *dual space methods* combining both approaches. Heavy atoms with large scattering power can be used to enhance the contrast and obtain better electron density maps as in the case of multiple isomorphous replacement (MIR). Phase information can be directly retrieved also by special methods exploiting resonant diffraction (multi-wavelength anomalous diffraction, MAD) and by high resolution transmission microscopy (HR-TEM); both MAD and HR-TEM are actually applied to limited cases, because they show severe practical limitations, especially in sample preparation and experiment execution.

Direct methods are founded on statistical relationship deriving from the positivity and atomicity conditions of the electron density. The resolution of the observed experimental reflections is therefore an important fact and pure direct methods work only with atomic resolution data (i.e. about 1 Å), and are mostly limited to small molecules. Unfortunately, atomic resolution data are often not

available in the case of protein crystals and of data from powder samples.[22] To overcome these limitations, real space and hybrid methods have been proposed exploiting the availability of computer power allowing fast Fourier recycling between the two spaces. In particular, simulated annealing methods in powder diffraction and dual space methods in protein crystallography have pushed forward the limits of crystallographic methods. In fact, structural problems that were impossible 10 years ago, such as protein structures with up to 10,000 atoms from single crystal diffraction, and small molecule structures from non-atomic resolution powder diffraction patterns,[34] can now be successfully sorted out. Although less stringent, data resolution remains an important issue for the success rate of the structure solution process.

It can be concluded that in all structure solution methods, signal to noise ratio, related to the quality and resolution of the experimental data, is the key point for a successful structure solution. In fact direct methods rely on statistical relationship and their number and reliability decreases as the signal to noise ratio decreases. Also in real space methods, the poorer the resolution, the more difficult is to identify the correct minimum, i.e. the correct molecular positions, in an already complex hypersurface, flattened by the low spatial and angular resolution limitation. In the particular case of powder diffraction, additional problems of peak overlapping and low 2θ resolution arise and phase retrieval becomes even more complicated as the signal to noise ratio is reduced. Besides, after successful structure solution, the retrieval of fine details in the electron density, such as light atoms close to heavy atoms, dynamic, static (e.g. adsorbed gases in microporous systems) and substitutional disorder, and is often limited by data resolution. Other intrinsic limitations related to the errors introduced by the truncation of Fourier series and by the limited contrast between signals (i.e. peaks from different elements in maps obtained from experimental data) and background, may also concur. As a consequence the obtained experimental electron density maps, Fourier difference maps or Patterson maps are always far from being perfect and show peak broadening and misplacement, together with spurious and negative peaks, making their interpretation often difficult and sometimes impossible. The particular application of the MED theory reported in the present paper is related to a potential solution of the "direct problem"[16] to obtain a clearer vision of the electron density of the most interesting part of the structure (i.e. the substructure responding to the stimulus), by selectively enhancing the signal of a subset of atoms (the active part, i.e. responding to the stimulus) and drastically increasing the signal to noise ratio, by suppressing the signals from the spectator (i.e. the part not responding to the stimulus). Also the experimental noise is reduced, because noise is in general spread on all frequencies while by PSD and PCA only the frequencies related to those of the stimulus (PSD) or to the main components (PCA) are analysed, suppressing all other terms. These results are obtained thanks to the post-experimental data treatment named "demodulation", which produces a pattern containing only contributions from the active substructure, to which standard crystallographic tools can be applied. Demodulation is carried out at first by PSD/Fourier filtering (§3.1.1) and then by an alternative method, recently implemented for MED, based on PCA (§3.1.2).

1.2 Description of a MED experiment

In general a sample exposed to a stimulus can be divided into two parts: an active part of the scattering density responding to the stimulus, and a spectator part remaining unchanged.[16] The simplest form of stimulus, from the experimental viewpoint, is a square wave, as in the case where a laser excites a sample by periodically switching on and off. This sequence is described pictorially in Figure 1 where MED parameters are defined. Before a MED data collection, the sample must reach a quasi-steady state equilibrium by a pre-treatment able to assure the reversibility of the response to the stimulus. For gas adsorption experiments the procedure consisted of an out gassing at high T, followed by isobaric adsorption at relatively low pressure, cooling and equilibration was carried out as described in the experimental section. This pre-treatment allowed the evacuation of the channels, by eliminating water and other adsorbed species, with all channels and adsorption sites available for the Xe gas, used for the MED experiment.

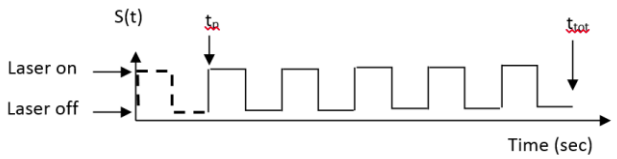

Figure 1: Square wave periodic stimulation with 6 periods. The first period is highlighted by a broken line for sake of clarity.

In a MED experiment, XRD data sets are collected as a function of time under a periodic stimulus of an external parameter with one cycle period of $t_p=2\pi/\Omega$ (Ω is the modulation frequency). In the case of powder samples, the data sets consist of one-dimensional diffraction patterns denoted by $A(2\vartheta,t)$. The main element of difference with respect to standard *in situ* experiments is that a single stimulus (broken line in Figure 1) is repeated periodically and identically for a large number of periods. Parameters of paramount importance are the number of repetitions (n) (for instance n = 6 in Figure 1) and the number (m) of experimental diffraction patterns collected per period. The periodic variation of the stimulus depicted in Figure 1 is named *S(t)*. In principle 3 datasets are enough to sample the stimulus effect and to collect the demodulated information[23], but to allow the best exploitation of modulation enhanced techniques for background suppression, n and m should be as larger as possible. Typically, the single pattern collection time (t_i) is much smaller than the stimulus period (t_p) and the overall experiment duration (t_{tot}) covers many periods of modulation. The n periods are then averaged (omitting the initial equilibration phase) into a single one to enhance the signal to noise ratio. In the following, we consider the response of the system $A(2\vartheta,t)$ as one averaged period. The two functions $A(2\vartheta,t)$ and *S(t)* may be correlated via a convolution integral to suppress the background and the scattering signals from silent species and to enhance the diffraction response connected to the modulated property.[16] More straightforwardly, $A(2\vartheta,t)$ may be processed at first by means of a demodulation integral, i.e. PSD (alternatively called "demodulation") as in ref. 23 and 24, but using directly the XRPD pattern, thus avoiding intensity extraction by Le Bail or

Pawley methods. We also showed that demodulation can be obtained by an alternative method based on Principal Component Analysis (PCA). PCA is a pattern recognition method that can be used for an effective representation of the system under investigation with a minimal number of new variables (called Principal Components - PCs). To our knowledge PCA was applied to qualitative[35] and quantitative[36] analysis from XRPD data, demonstrating its power in retrieving information hidden in large amounts of data. PCA is in general applied as an analytical tool, while we propose for the first time its application to solve crystallographic problems related to structure solution. PCA can be very useful in investigating data quality, speeding up the data analysis and reducing or eliminating data pre-treatment, required by PSD. Both demodulation methods (PSD and PCA) allowed obtaining a demodulated pattern, treatable by standard crystallographic software's, to obtain the substructure of the active atoms (Xe in our case), suppressing the signal of the static part of the structure (i.e. the zeolite). The two approaches of post-experimental MED data treatment (PSD and PCA) are applied to the simulated (§3.1) and experimental (§3.2) data. Finally, PCA and PSD potentialities and limitations are discussed (§4).

2. Experimental

2.1 Sample preparation and in situ experimental setup

Ga-MFI was synthesized as in ref. 4. Template removal was carried out by thermal treatment at 800 K in air. The sample was then ground and inserted in a capillary between two glass wool flocks. The capillary was then fixed through a T-piece to a gas/vacuum line. Quasi steady-state equilibrium must be reached before starting the MED experiment. To assure this, an equilibration process of the sample was carried out and monitored by collecting XRPD patterns. The sample was at first out gassed at 423 K to remove air moisture from the zeolite channel, then cooled at RT and filled with Xe at the pressure of 0.14 bar. The sample was finally cooled to 200 K by a cryostream and the equilibrium was reached as indicated by no further changes in the collected XRPD patterns. Then repeated heating/cooling cycles were carried out and the process resulted fully reversible and each cycle identical to the previous one, within the experimental error.

2.2 Data collection

X-ray powder diffraction experiments were performed at the ESRF in Grenoble at the SNBL beam lines.[37] Static high resolution XRPD data and preliminary MED data were collected by the standard high resolution BM1B setup[38] using both MAR345 and Pilatus 300K-W detectors. In situ XRPD data of high spatial and reciprocal space resolution were finally collected at BM1A with a PILATUS@SNBL diffractometer using a Pilatus 2M[39] detector.
Preliminary static high resolution data were collected at RT, after evacuating the sample with Xe pressures of 0.14, 0.4, 1, 3, 10 bar. These data indicated that 0.14bar is the upper limit for a full desorption and absorption within 200 and 400 K. Therefore T-MED data were collected at constant pressure of 10 and 100 mbar, and P-MED within 90 and 150mbar. Table 1 summarizes the conditions of the performed MED experiments

Varied parameters	Min values	Max values	Amplitude
T1 at 0.140 mbar	200 K	400 K	200 K
T2 at 0.140 mbar	300 K	340 K	40 K
T3 at 0.140 mbar	310 K	330 K	20 K
T4 at 0.140 mbar	320 K	330 K	10 K
P1 at 278 K	90 mbar	150 mbar	60 mbar
T5 at 10 mbar	200 K	300 K	100 K
T6 at 100 mbar	200 K	300 K	100 K

Table 1: Conditions employed in the MED experiments.

2.3 Generation of simulated data

A simulated experiment was designed and realized to test the proposed MED approach for the "direct problem" solution,[16] in the case of powder diffraction data, by generating a set of diffraction data, using the TOPAS software.[40,41] An MFI zeolite system, containing channels that can absorb gases, was employed as test sample. In particular, a Xenon containing calcined MFI zeolite framework was chosen, where the framework represents the spectator species and Xe in the channels represents the active species. The modulation experiment is carried out changing the occupancy of Xe atoms between the extreme points represented by i) channels fully filled with Xe occupancy equal to 1.0 and ii) channels completely void with Xe occupancy equal to zero. The starting model was therefore a zeolite with Xe atoms inside the channels, and their number and positions was obtained from the solution and refinement of the static (constant room temperature and 10 bar pressure) diffraction pattern of the sample with the highest Xe content. In the simulated experiment the virtual applied stimulus causes the periodic desorption and absorption of Xe atoms from the channels. Theoretical powder patterns where therefore calculated changing the occupancy of the Xe atoms from 0 to 1, following the procedure described in ref. 24. This corresponds to set a=b=1/2 in eq. SI-7 of the ESI file. Two stimuli shapes are applied, the first being the simplest from the mathematical viewpoint, i.e. a sinus variation (identical to that described in §4.2 of ref. 16) and the latter the simplest from the experimental viewpoint, i.e. a triangular variation. Xe adsorption induces large changes in all the XRPD pattern, but low angles peaks represent the finger print of channel content, with high and low intensities observed with empty and full channel respectively, as a consequence of the increased electron density in the channels resulting in destructive interference. The "triangle simulation" data show at first glance the expected effect of depleting, with a triangle-like trend, low angle peaks at high Xe occupancy.

2.3 Demodulation by phase sensitive analysis

Phase sensitive detection was applied to demodulate MED data. The equations outlined in the ESI file, §1, were applied, and showed that the sample intensity response of double frequency with respect to the stimulus frequency, contains the structural information on the active species only. A script in MATLAB[42] was written to implement the following procedure:
- the set of powder patterns collected during the experiment are averaged in time over the periods of the stimulus;
- the resulting $A(2\vartheta,t)$ matrix is transformed to the $A_k(2\vartheta,\phi)$ matrix by using eq. S3 in the ESI file. This operation is repeated for k=1 and for k=2;
- the most suited values of in-phase angle ϕ are chosen by looking

at the maxima in the functions $A_1(\phi)$ and $A_2(\phi)$, using the so called in-phase angle plots;
- the decomposed patterns correspond to the vectors $A_k(2\vartheta)$ obtained by projecting the matrix $A_k(2\vartheta,\phi)$ over the selected in-phase angle values.

Results of the procedure for simulated data are shown in Figures SI-1 (ESI file) and for experimental data with large T window in Figures SI-2, SI-3 and SI-4 (ESI file). MED data with smaller T variations showed better agreement with simulated data and the results are discussed in §3.2.2.
For real data, when the applied stimulus is not periodic, such as in the case of a simple temperature ramp, raw XRPD data can be treated only by PCA to obtain the demodulated pattern. To treat a simple ramp by PSD demodulation, a mirroring procedure was applied to generate periodic "MED-like" data from single ramp data. The PSD procedure was then applied to mirrored data and the demodulated pattern obtained.

2.4 Demodulation by principal component analysis

PCA, as implemented in the program RootProf,[43] was used to carry out demodulation in alternative to PSD. For comparison PCA was also carried out with standard PCA software *Unscrambler*.[44] Input XRPD patterns were arranged in a data matrix, having 2θ values as columns and diffracted intensities as a function of T or P in rows. The order of the patterns in the data matrix does not affect the PCA analysis. Data were pre-processed by standard normal variate along columns, i.e. the intensities of each pattern were rescaled to have zero mean value, and divided by their standard deviation. In all the considered cases the two first principal components (PC1 and PC2) explain about 90% of the total data variability (about 70% for PC1), as shown in §3.1.2. The score and loadings of the first two principal components were taken as output. The scores represent the extracted time dependence of the data, the loadings the corresponding XRPD intensities.

3. Results

3.1 Results on simulated MED data

3.1.1 Demodulation by Phase Sensitive Detection (PSD)

The demodulation procedure as outlined in §2.3 has been applied at first to simulated data (Figure SI1-a). Instead of applying the MED approach after extracting intensities by Pawley or Le Bail methods as in ref.24, the MED approach was here applied directly to the simulated powder patterns and phase sensitive detection was carried out. The PSD results were in full agreement with the theoretical expectations: in-phase angles of 0° and 180° were found for the demodulation at the same frequency Ω of the stimulus (case *k*=1), while the in-phase angle 270° was found for the demodulation at 2Ω (case *k*=2) as can be seen in Figure SI1b and c. In both cases single in-phase patterns were obtained which, according to the theory, coincide with powder patterns. (see Figure 2).

3.1.2 Demodulation by Principal Component Analysis (PCA)

PCA was used to unravel trends in the MED data. The loadings of the first two principal components (named PC1, PC2) are related to the demodulated pattern obtained by PSD. In particular, PC1 resulted almost identical to the 1Ω demodulated pattern by PSD (Figure 2a), while PC2 was only similar to the 2Ω demodulated pattern (see figure 2b). In the ideal case in which changes in the Xe occupancy are the only effect of the T/P modulation (eq SI-6 in ESI file, § 1) shows that the time dependent terms in the observed amplitudes are $|F_A(t)|^2$ (i.e. 2Ω) and the cross term $F_A(t)F_S^* + F_A^*(t)F_S$ (i.e. 1Ω). The former has only contribution from Xe (Active) atoms, while the latter has contribution also from the zeolite framework (silent spectator) atoms, and is therefore much larger than the first.

(a)

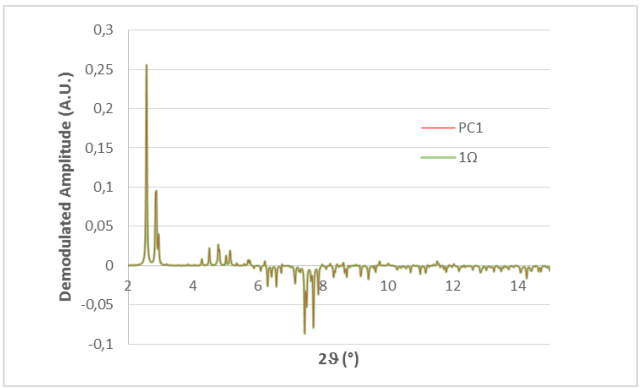

(b)

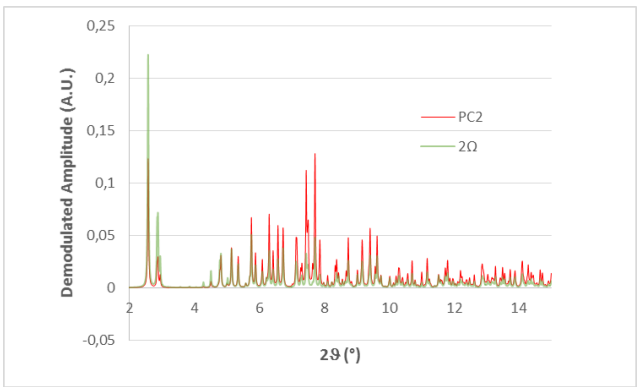

Figure 2: Comparison of demodulated amplitudes (a) at 1Ω and PC1 by PSD and PCA analyses respectively, and (b) at 2Ω and PC2; PCA and PSD data were scaled using a scale factor calculate on the full pattern intensities.

The function describing the time dependence in the former term is squared with respect to the same function in the latter term. The PCA extracts trends from data, hence neglects the time-independent term $|F_S(t)|^2$ in eq. SI-6, assigning the highest time-dependent changes to PC1 and the residual changes to PC2. Therefore PC1 is expected to hold contribution from the mixed active-silent atom term, while PC2 retain the sole contribution from active atoms. This explains the fact that the PC2 scores and 2Ω are all positive (Fig.2a), while the PC1 scores and 1Ω can have negative peaks due to the interference between active and silent substructures (Fig.2b), according to MED theory.[16] These hypotheses can be checked by looking at the trend of the PC1 vs PC2 scores (Figure 3b). They reproduce the expected time-dependence of mixed terms (PC1, with the same frequency of the stimulus, thus with the same trend of 1Ω from PSD) and active

terms (PC2 with double frequency with respect to the stimulus, thus with the same trend of 2Ω from PSD) (Figure 3a), and satisfy almost exactly the expected condition: $PC2=PC1^2$, as shown by the scatter plot of PC2 vs. $PC1^2$ generated by RootProf (see Figure 3b). The almost linear correlation confirms that PC's follow the same trend of 1Ω and 2Ω but with some deviations from the PSD demodulation Summarizing, it is already impressive how well PCA is able to extract, in a much faster and simpler way, the PC1 loading and scores corresponding to the 1Ω component. Conversely, PC2 loadings and scores do not match completely the 2Ω intensities (even though peak shape and position are correctly retrieved), and more work is needed to improve PC2 extraction.

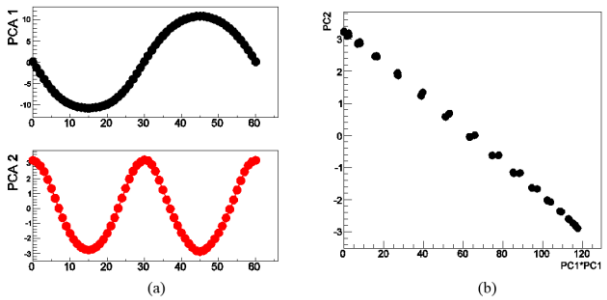

Figure 3: Scores of the first (PC1) and second (PC2) principal components: separate plots vs. dataset number (a), and scatter plot of PC2 versus PC1*PC1 (b).

The differences between PSD and PCA demodulation methods were evaluated quantitatively by calculating the Pearson's correlation coefficient (Corr in Table 2) and the internal agreement factor (Rint as known in cystallography).[45]

From the crystallographic view point, despite a medium (75%) correlation, Rint between PC2 and 2Ω is smaller than 42,6%. The discrepancy appears rather big but it is concentrated in the low angle peaks ($2\vartheta = 2.8°$ in Figure 2b). In fact, excluding the two peaks at $2\vartheta < 3°$ the correlation between PC2 and 2Ω goes to 90% and the Rint down to about 20%. This reduced discrepancy allows solving the substructure solution by standard routine direct methods by PC2 loadings, as detailed in section 3.1.3. Even if the two patterns in figure 2b appear different and their correlation is not high, they mainly differ in the two low-angle peaks. In fact, by excluding these two peaks the correlation between 2Ω and PC2 reaches 90%.

Comparison	Corr	Corr(*)	Rint	Rint)*)
PC1 vs 1Ω	0,999983	0,999975	1,18%	1,42%
PC2 vs 2Ω	0,75	0,90	42,6%	27,6%
PC1(RP) vs PC1 (US)	1.0	1.0	0.0%	0.0%
PC2(RP) vs PC2(US)	1.0	1.0	0.0%	0.0%

Table 2: Agreement and correlation calculation between PCA and PSD demodulation methods and between PCA analysis carried out with *RootProof* (RP) and *The Unscrambler* (US); Corr(*) and Rint(*) are calculated excluding the two more intense low angle peaks.

As well known, low-angle peaks are often not collected because of beam-stop problems or obtained with very wrong precision, because of absorption and/or optic problems, and their absence or incorrectness is not detrimental for a successful structure solution. This considerations explain why PC2 and 2Ω can both be used to obtain the Xe substructure, despite they are quite different. As a general comment, the incorrectness of PCA with respect to PSD on simulated data is small in absolute value and affects differently PC1 and PC2. PC1 counts for more than 95% of the data and the error is quite small on PC1 absolute intensity and affects only its baseline (see figure SI-1d in ESI file where PC1 vs 1Ω discrepancy is highlighted by scaling on the intensity of larger peak). Conversely PC2 represents only the 2% of the data and its intensity is of the same order of the error that is much larger (figure 3b). The efficiency and precision of PCA of recovering the same information of PSD is schematized in Figure 4, where horizontal rows indicate relation between demodulated profiles and PCA loadings, vertical rows indicate the relation between time-dependent trend and PCA scores. However, it should be noted that PSD cannot be applied in case of non-periodic stimuli, or non-linear response.[15] These arguments allow us to propose PCA as a fast and efficient demodulation method for systems with unknown response and subjected to non-periodic perturbations e.g. ramps, that are much simpler to be experimentally obtained with respect to periodic stimuli (figure 1).

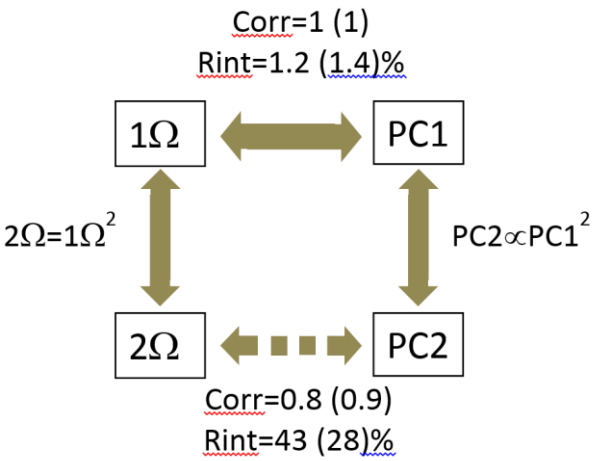

Figure 4: Schematic view of the relation between PCA and PSD demodulation. Horizontal rows indicate relation between demodulated profiles and PCA loadings, vertical rows indicate the relation between time-dependent trend and PCA scores. Agreement estimated by correlation (Corr) and internal agreement (Rint) on all data and excluding low angle peaks (in parentheses).

3.1.3 Crystal structure solution by direct methods from demodulated patterns

The pattern obtained by plotting demodulated amplitudes at 2Ω vs. 2θ was chosen for substructure solution and refinement because, according to the MED theory, it is expected to contain only the diffracted intensity from the active sublattice, i.e. of Xe atoms. A visual inspection confirmed that the 2Ω demodulated pattern from simulated data (Figure 5) appears as a normal XRPD pattern and was thus treated by a standard structure solution procedure. The first test was carried out on peak positions, resulting in complete agreement with the known cell of TSI-1 zeolite. Then *ab initio*

structure solution was carried out by the EXPO software,[46] employing its standard direct methods procedure on extracted intensities. Only the lattice parameters and the expected atomic content were given as input and a solution was found in few seconds, showing the highest peaks in positions corresponding to those of the Xe substructure (the active part of the experiment). The pattern was then refined, optimizing peak profile and background functions and a complete agreement with the simulated data was found (violet line in Figure 5) with rather good R value (Figure SI1-e in ESI file). Conversely the zeolite framework, perfectly silent in this simulated experiment, does not show any signal in the pattern obtained by demodulating the data at 2Ω.

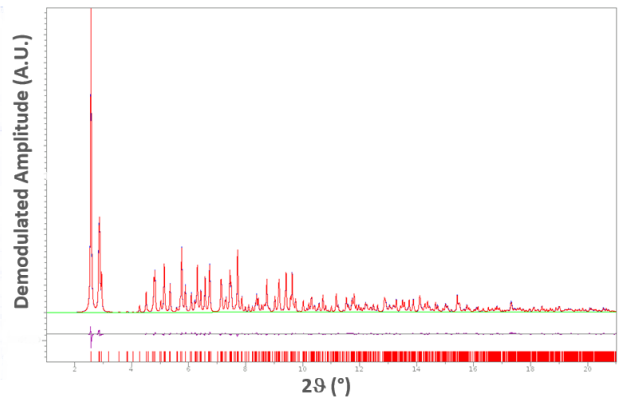

Figure 5: (a) 2Ω demodulated pattern obtained from simulated data (blue) and calculated pattern resulting from Rietveld refinement of the best phasing solution (red). The difference pattern is shown in violet; (b) evolution of the agreement factor between observed and calculated profiles (Rwp) during the refinement procedure.

The theoretical predictions of ref. 16 have been thus verified in a simulated experiment, i.e. MED allows the structural analysis of the active sublattice (Xe) with a complete suppression of the spectator signal (the zeolite framework). This assessment by a simulated experiment was very helpful in designing the real world experiment and checking and optimizing experiment execution and data analysis. Under certain boundary conditions explained in paragraph 3.2.1, any molecule, the electron density of which can be selectively varied in an *in situ* XRPD experiment, can be selectively probed from the diffraction viewpoint, thus showing the unprecedented chemical selectivity of MED. From a theoretical point of view this selectivity is not due to the fact that Xe is a heavy atom, and can be in principle applied to any chemical species from lighter ones like hydrogen to more complex ones as molecules. As explained in the next section, due to the signal to noise limitations, in practice, the amplitude of the induced stimulus plays an important role and does depend directly on the number of electrons varied (ref 23).

3.2 Results on experimental MED data

This section deals with the attempts at executing a real MED experiment to reproduce the simulated one with the dual aim of understanding technical problems related to the experiment execution and to obtain more hints on the feasibility of a "real world" MED experiment. At first the most successful MED experiment is presented, then the various possibilities of modulating the electron density are presented in order to highlight advantages and drawbacks for the practical application of MED for phasing, i.e. for solving the direct problem.

Two parameters (pressure or temperature) can be experimentally varied to induce the occupancy modulation of Xe atoms used in the simulated experiment (§3.1), without, in principle, affecting the framework, that is the silent spectator. Moreover the amplitude of the stimulus can be varied by a large amount, modulating Xe from minimum (i.e. zero) to maximum occupancy (i.e. up to about 0.5-1.0) depending on Xe site and on the Xe pressure (see figures SI-6 and SI-7 in the ESI file for a detailed discussion on the implications of changing the stimulus amplitude), as found experimentally after static MFI refinements of T1 dataset by Topas[41] software, yielding to occupancy values different in different sites and differing from the theoretical value of 1, used in the simulated experiments. Using a lower pressure the situation is closer to the simulated conditions (less crowding in the channels and reduced chemical interactions, negligible variations of the zeolite framework), but full occupancy cannot be reached. At higher pressure, full occupancy is reached but the occupancy vs. T behavior is more complex and far from being linear or sinusoidal (as detailed in section 4.3).

3.2.1 MED experiments

Realizing a real occupancy modulation MED experiment with results identical or similar to those of a simulated one, requires, on one hand, overcoming technical difficulties such as applying a periodic stimulus, which is synchronized with the data collection procedure. On the other hand, the boundary conditions of the MED theory have to be approached in practice. These are linearity of the response, absence of lattice variations, absence of other atom-related variations (in positions, ADP's and structure factors) and absence of kinetic effects and hysteresis in sample response. In an attempt to fulfill all these requirements in "the real world samples" several experiments have been carried out, in isothermal and isobaric conditions, as detailed in Table 1. Figure 6 depicts the logical path followed in the data collection optimization highlighting the problems and the proposed solutions.

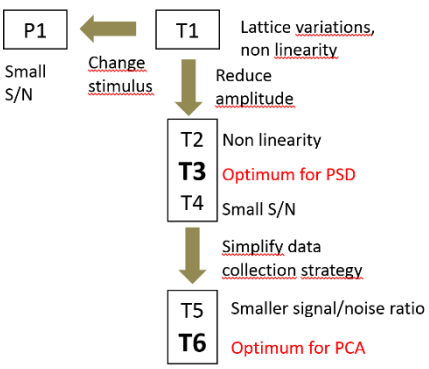

Figure 6: Summary of the procedure used to reproduce experimentally the MED theory. In bold the «best MED experiments» descripted in details in §3.2 (PSD) and 3.3 (PCA).

Among all experiments in Table 1, T3 and T6 resulted the best experiments (as highlighted by bold characters in Figure 6) for PSD and PCA analyses respectively, and are fully described in this paper, while details on the other experiments are summarized in §2

and 3 of the ESI file. After the preliminary static measurements of MFI loaded with Xe at pressures varying from 10 bar down to 0.1 mbar, temperature modulation was at first used, adjusting the static pressure of Xe to a value (0.14 bar at 273 K) such that a temperature modulation from 200 to 400 K (Figure SI-2 in ESI file) allows a full evacuation (at 400K) and a complete filling (at 200 K) of the channels. A symmetric triangular stimulus shape was used, because it's much simpler to create from the experimental viewpoint with respect to a sinus one. As long as the stimulus shape is symmetric the MED theory will hold; symmetric functions can be decomposed in in a sum of odd harmonic terms of frequency multiples of the frequency Ω of the triangular wave. This was also confirmed by a simulated experiment with a triangular-shaped stimulus. Three cycles were carried out and 40 XRPD datasets per pattern per cycle were collected. Since the large amplitude stimulus causes violation of the MED assumptions (non-linearity between stimulus and response and also lattice variations), the demodulated experimental pattern resulted different from the simulated one (see Figure SI-5 in ESI file). In Figure SI-8 the non-linear response to a triangular stimulus is evident from the sinus-like variation of Xe occupancies (Red and black lines) vs. temperature. However a limited region (highlighted by the green ellipse in figure SI-8) with a linear response can be found and smaller amplitude experiments designed. To follow the blue line in Figure SI-8, experiment T2, T3 and T4 were carried out. It must be noted that the effects of reducing the stimulus amplitude were studied also in a simulated experiment (Figure SI-6), indicating that in theory no signal to noise reduction should be observed. The experiment T3 (Figure 7) resulted the best one in fitting the PSD theoretical conditions. It must be mentioned that also pressure modulation was tested (experiment P1 in Table 1). P modulation (Figure SI-9 and §4 of ESI file) resulted fine in reducing lattice variations, but the pressure range available was too small to achieve a relevant stimulus of the sample. A larger range pressure modulation experiment on MOFs was recently reported,[47], adopting a similar MED approach.

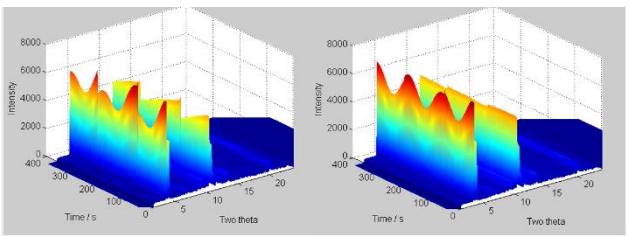

Figure 7: Real MED data powder diffraction data on Xe occupancy variation inside a TS-1 zeolite, by a triangular small amplitude stimulus (experiment T3 in Table 1), before (a) and after (b) normalization toward beam decay.

3.2.2 The small temperature window modulation experiments

Small T windows (10, 20, 40 K) were explored in experiment T2, T3 and T4, the smaller the T window the smaller the stimulus in the MED experiment. In principle the smaller the stimulus, the smaller the lattice variation and the deviation from the linearity of the response. Unfortunately, the S/N ratio is expected to be smaller in the real world, while in simulated experiments the amplitude of the stimulus only applies a scale factor to the data (Figure SI-7). The 20 K window experiment (Figure SI-10) resulted the best compromise between S/N ratio and compliance to MED boundary criteria. Figure SI-8 in ESI file (Occupancy of Xe atoms vs. T) explains why the small T windows allow obtaining reliable data. As a consequence, the b parameter in eq. (SI-7) is reduced. These temperature windows allowed obtaining a triangular intensity modulation similar to the stimulus since the 1Ω term is dominant (more than 90%). Then the 20 K windows was chosen to maximize signal to noise ratio. The demodulation procedure carried out on 20 K window data resulted in in-phase angles and 2Ω demodulated patterns encouragingly similar to the simulated ones and was used for structure solution and refinement (Figure 8). As expected, the 2Ω demodulated pattern showed mainly positive peaks similarly to the simulated experiment. The pattern was therefore employed for structure solution with the EXPO software: the indexing was successful, with a resulting cell in agreement with the cell of a TSI-1 zeolite and a solution with 4 Xe atoms located in the MFI channels was found, even if the fit and profile agreement values were not as good as in the simulated experiment. Also peak positions resulted approximated and the ADP's were larger (20-40 instead of 3-8 Å^2) than expected for a well refined structure.

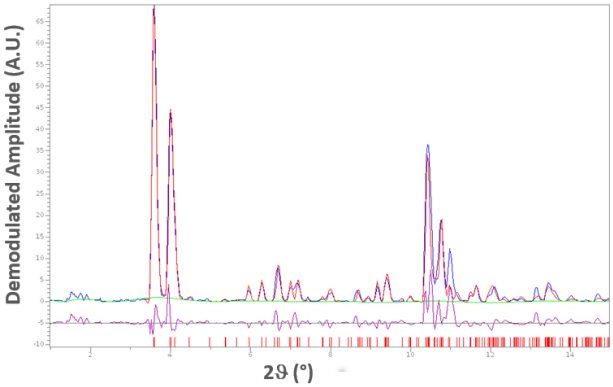

Figure 8: Rietveld refinement of the best phasing solution (red) using the 2Ω demodulated pattern obtained from real data with a 20°K T window (blue). The difference pattern is shown in violet.

3.3 Analysis and demodulation of MED experimental data by PCA

3.3.1 PCA on non-periodic (ramp) experimental data

The PCA analysis was carried out on T1-T6 experiments, by assuming that PC1 and PC2 loadings are related respectively to 1Ω and 2Ω patterns obtained by PSD analysis (see §3.1.2). The results of the best PCA experiment (T6 as detailed in figure 6 and its discussion) are reported in the present paper, while other results on other dataset are reported in the ESI file §5, for sake of completeness. PSD demodulation cannot be applied directly to raw T5 and T6 data (figure 9), because the applied stimulus was a simple not periodic temperature ramp, and refinement of static data has shown that Xe occupancies follow a non-symmetric increasing trend (Figure 10). PCA analysis of T1-T4 data was carried out analyzing PC1 vs. PC2 plots. The expected parabolic relation as in simulated data (Figure SI-11a and b) can be recognized in experimental patterns (figure SI-11c and d) but it is very poor for T3 data (Figure SI11-c), because of the already discussed problems (lattice variations and/or small signal/noise ratio). T6 experiment shows the best approximation of the expected behavior (figure SI11d) and this experiment is thus described in detail in the

following section.

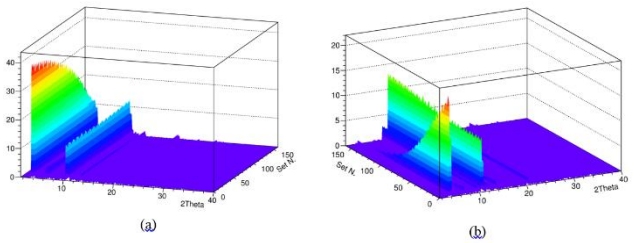

Figure 9: XRPD ramp data with Xe occupancy variations, induced by a T ramp from 300 to 400 K with a pressure of 10 (a) and 100 (b) mbar; the temperature is linearly increasing from 300 K (full channels and low intensity of low angle peaks) to 400 K (empty channels and high intensity of low angle peaks) from set n. 150 to set n. 0.

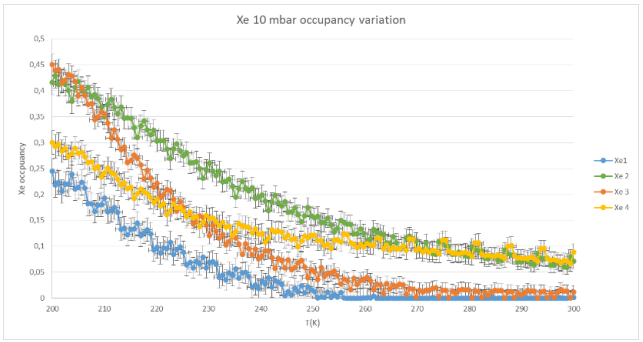

(a)

(b)

Figure 10: Xe occupancies in 10 (a) and 100 (b) mbar data vs temperature (T5 and T6 experiments), i.e. response of the system vs. the stimulus.

The score plot for the T6 experiment (Figure 11) indicates that the PC1 scores reproduces the average trend of Xe occupancy of Figure 10, and the PC2 scores are roughly equal to PC1*PC1. It is worth noting that a significant PC3 component was found in this case, resulting in an oscillation of zero error due to the experimental setup. As a consequence, the linear trend in the PC2 vs $PC1^2$ plot (Figure 11b) is not perfect as in the theoretical case (Figure 3) , and periodic oscillations are present in the PC2 scores. Such an effect is even more pronounced in data from the T5 experiment, due to the lower signal from Xe occupancy. This small and in some case problematic feature was not seen during experimental data collection, by standard "real time" data check such as visual inspection of the pattern and fast refinement of some static XRPD pattern. Conversely PCA can, in the future, be used to check and validate data while the experiment is running, thus becoming also a precious tool for experimental strategy optimization. This could lead to a much better exploitation of synchrotron beam time. Interestingly, PCA can be easily applied to any subset of XRPD experimental patterns, either varying arbitrarily the amplitude of the stimulus of the experiment, or simply using data selected in a restricted temperature ramp. This allows selecting the condition where the S/N ratio is larger and the variations of the active atoms more evident and thus more easily detectable.

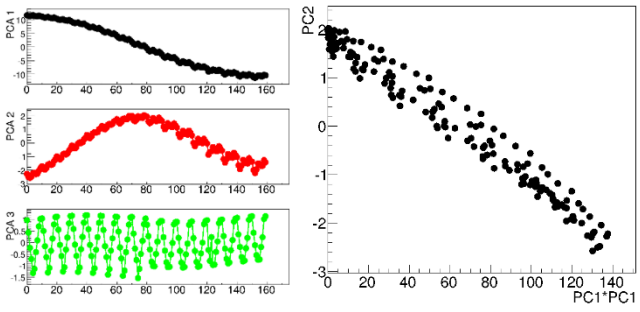

Figure 11: Scores of the first (PC1), second (PC2), and third (PC3) principal components for 100mbar data (T6 experiment): separate plots vs. dataset number (a), and scatter plot of PC2 versus PC1*PC1 (b).

PC2 loadings were treated as a standard XRPD pattern and solution of the substructure was attempted by EXPO. The pattern obtained plotting PC2 loading vs. 2ϑ (figure SI-12 in ESI file), despite being more noisy and with incorrect intensities with respect to the PSD-demodulated plot (Figure 7) still appears as a standard XRPD pattern (with correct peak position). The two patterns obtained by plotting PC2 vs. 2ϑ of experiment T5 and T6 were treated by EXPO software to evaluate their information content, and the results of the refinement of T5 case is reported in Figure SI-12. Despite the not fully correct intensity extraction by PC2, the observed Xe substructure can be partially retrieved locating 2 out of 4 Xe atom in the channels and the pattern roughly refined (Figure SI-13).

4. Discussion

4.1 Advantages and drawbacks of different experimental methods and data analysis for a real MED experiment

Reproducing "in the real world" the simulated occupancy variation test was not straightforward because some crystallographic parameters are correlated, making very difficult or impossible to design an experiment where the response to an external stimulus affects a single variable. Moreover, the MED theory is strictly valid only if the sample responds linearly to the stimulus, as discussed in details in Chernyshov *et al.*[15] However gas absorption and desorption in a zeolite framework is a "real world" scientific case, quite far from being a linear phenomenon, because of the lack of homogeneity of the active sites, the non-reversible behavior, and the presence of relevant kinetic effects. Although Xenon is a noble gas, so that these effects should be limited, saturation at high loadings and specific chemical interactions among Xe atoms and metal ions and/or defective sites into the zeolite framework, are unavoidable problems. A non-linear response introduces

additional 2Ω components due to the influence of the shape of the function in the Fourier series expansion hence contaminating the 2Ω contribution from the active sublattice, while under the linear response approximation the demodulation process is straightforward and the expected results are identical to those of the simulated experiment. To approximate such ideal behavior, different ways of imposing the stimulus have been explored, using both T or P stimulus and, in the most promising case of T-MED with different stimulus shape and amplitude (see Table 1 for the summary of the more successful experiments) structure solution and refinement were successful. Concerning data analysis and substructure retrieval, two methods, PCA (exploiting variance analysis) and PSD (based on Fourier analysis) were used. The decomposition by PSD resulted successful in the simulated case, and with some technical difficulties, satisfying from the experimental viewpoint. The decomposition by PCA is intrinsically approximated, since the principal components could be in principle constituted by a mixture of first and second harmonics of a FFT expansion, hence of 1Ω and 2Ω signals from PSD, as a result of a compromise between orthogonality among eigenvalues and maximization of data variance. In our specific dataset, this is definitively not the case for the first principal component, which captures very well the 1Ω PSD signal, while the second component is somehow affected by such a limitation..

Demodulation procedure requirements and capabilities

	PSD	**PCA**
Periodic stimulus	YES	Not necessary
Normalization/background subtraction	YES/YES	YES/NO
Error detection	NO	YES

Feature retrieved in the demodulated patterns

		PSD	**PCA**
1Ω/PC1	*Peak position*	YES	YES
	Peak shape	YES	YES
	Peak intensity	YES	YES
2Ω/PC2	*Peak position*	YES	YES
	Peak shape	YES	YES
	Peak intensity	YES	NO

Table 3: Comparison of PSD and PCA approaches to analyze MED data.

As summarized in Table 3, PCA outperform PSD in term of easiness of use (a simple T ramp is enough to obtain demodulated patterns) and ability of detecting anomalies in data collection, but still is not able to recover correctly the 2Ω term to solve the active substructure.

4.1.2 Effect of the stimulus amplitude on simulated and real data

PSD analysis resulted affected by the experimental conditions. The effect of the stimulus amplitude was explored in a simulated experiment modulating the occupancy from 0.25 to 0.75 instead than from 0 to 1, with sinus stimulation. The simulated data in the two ranges gave the same results, except for a scale factor, as shown in Figure SI-5 and SI-6. In fact the scale of the 2Ω demodulated pattern of the simulated dataset is dependent on the occupancy variation, i.e. on the stimulus amplitude. Being the simulated data "error free", there is no information loss when diminishing the stimulus amplitude. In real data, being the noise constant, the signal to noise ratio in the experimental 2Ω demodulated pattern becomes smaller when the temperature window, i.e. the stimulus amplitude, decreases. Indeed the 20 K T window resulted a good compromise, being small enough to limit the problems due lattice variation and non-linear response of the sample, but large enough to selectively detect the diffraction signal coming from the active sublattice, thus allowing the structure solution of the Xe crystal structure, i.e. of the active species.

4.2 The MED experiment procedure

The experimental "real world" reproduction of the simulated MED experiment for the direct problem solution[16] in all the key steps (data production, demodulation at 1Ω and 2Ω, and the exploitation of the file for substructure solution) was attempted with different approaches. The first step, i.e. obtaining several modulated diffraction dataset, with enough cycles and collected XRPD patterns was straightforward. In fact, a large or small Xe occupancy variation was induced easily at isothermal (pressure modulation) or isobar (temperature modulation) conditions. The second step, demodulation to obtain a useful 2Ω demodulated XRPD pattern was the most complicated step. In fact in most cases (about 20 experiments were carried out to produce the fully analyzed dataset in Table 1), the resulting data were not useful after demodulation, because of a combination of parameter correlations (correlation of occupancy with lattice variations was the main problem) and violation of the linear response approximation (eq. SI-13), which is, at the moment, the only one available from the theoretical viewpoint.[16] However, the adjustment of the conditions in isobaric experiments (small T amplitude experiment) allowed to limit the experimental problems due to parameter correlations, lattice variations and non-linear response, and 2Ω demodulated pattern suitable for substructure solution with standard crystallographic methods (EXPO software) could be obtained.

Moreover, advantages and drawbacks of the various approaches employed in this paper were analyzed. The main advantage of pressure modulation over temperature modulation, for the "direct problem" solution[16] is the observed very small lattice parameter variation during the isothermal experiment. In fact a large amplitude of the stimulus in the temperature modulation experiment hampered demodulation not only because of the non-linear response effect, but also because of the unit cell variations, that affect Bragg peak positions. In fact, demodulation of the XRPD dataset became non-sense, since the demodulation procedure does not take into account at all peak position, but treats each data point in the pattern singularly. One possibility of overcoming the lattice variation issue is by treating large amplitude temperature datasets, exploiting a peak extraction procedure (with Le Bail or Pawley methods) on raw data. In this way it is possible to obtain a set of experimental (hkl) amplitudes modulated as a response to the stimulus and then apply the demodulation procedure to obtain a 2Ω demodulated set of (hkl) amplitudes to be analyzed with a single crystal structure solution and refinement software.[24]

The datasets not useful for the solution of the direct problem are very useful for the inverse problem,[16] i.e. the analysis of the kinetics of adsorption/desorption process. In fact their usefulness for the demodulation at 2Ω resides mainly in the violation of the non-linear response approximation, which is related to the chemistry of the system, namely to: i) different positions of Xe with different occupancy (correlation between occupancy and position); ii) different adsorption energy at different temperatures, inducing different speed of adsorption and desorption at different T/occupancy; iii) hysteresis effects between adsorption and desorption.

These deviations from the linear response are detrimental for the solution of the direct problem, but contain very useful information for the adsorption/desorption process, a key step in many scientific and technological problems.

4.3 The behavior of Xe inside MFI channels

Thanks to the combination of static refinements and MED analyses, Xe atoms were located and the chemistry of Xe sorption and desorption was investigated. Four adsorption sites (Table 4 and Figure 12) were found independently by simulated annealing using static data and by EXPO analysis (Figure 8) of demodulated patterns. Xe1 and Xe2 are located at the center of the straight channel. Xe3 and Xe4 are close to the center of the sinusoidal channel. Xe-O distances are in the range 3.93-4.60 Å, i.e. larger than 3.58 Å, the sum of Oxygen and Xenon vdW radii, and therefore suggesting for Xe a gaseous-like situation. These results represent an improvement with respect to previous work by Torigoe et al.,[30] who studied the structure of Xe inside a Cu-MFI by XAS and theoretical calculations with the cluster approach. They obtained precious information on Cu-Xe distances and local Xe structure, but the experimental Xe positions in the unit cell (Table 4) could be obtained only by XRD. Indeed among the four position found by MED analysis, Xe1 and Xe2 (Figure 12) are in a position similar to that inferred by Torigoe et al. (see figure 4 in ref. 30). This similarity suggests that Ga atoms (present in our samples) can interact with Xe similarly to Cu, thanks to its ability of polarizing Xe electron density.

Xe atom coord.	x	y	z
Xe1	½	¼	0
Xe2	½	0	0
Xe3	0.311(1)	¼	0.819 (1)
Xe4	0.103(1)	¼	0.855(1)

Table 4: Experimental Xe atom positions.

Analyzing the occupancy variations as a function of the thermal stimulus, the information about the different stabilities of the various sites was obtained. Moreover the deviations of the experimental MED data from theoretical expectations and simulated experiments, allowed to further investigate the Xe adsorption behavior, that resulted far from being ideal, with kinetics effects playing a major role, despite the noble gas behavior of Xe.

The different behavior of the four Xe atoms during the thermal treatment (Figure 10) is surely related to their different chemical environment, due to the different size of the sinusoidal and straight channels. This aspect represents a deviation with respect to the simulated experiment, where the Xe atoms respond to the stimulus in the same way and the four occupancies vary accordingly. Conversely in the real case, the Xe occupancies vary independently one from the other and this can affect the demodulation efficiency, introducing spurious components in the 2Ω channel. On one hand this behavior explain the difficulty of reproducing experimentally the simulated MED experiments. On the other hand, MED was useful to highlight the features of Xe adsorption into MFI channels.

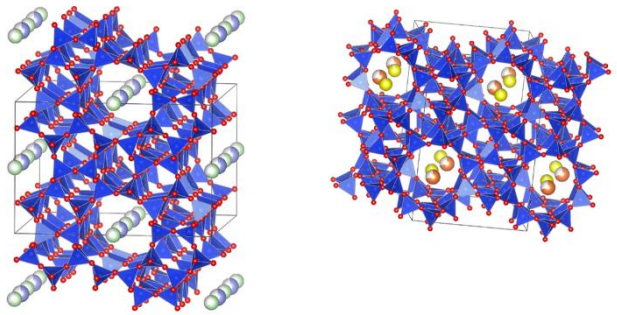

Figure 12: Location of Xe atoms into straight (a) and sinusoidal (b) channels of MFI zeolite (X1 blue, Xe2 green, Xe3 orange, Xe 4 yellow).

While the occupation of Xe atoms varies with temperature, their positions remain rather constant when varying either T (MED experiments) or P (static experiments). This aspect is in agreement with the MED assumption of variations of only one parameter (occupancy) as a response to the stimulus (temperature). However the thermal parameter varies during MED experiment, with Xe being more disordered as the temperature increases. In fact, Xe atoms resulted disordered in the channels, as indicated by the high values of the B-factors observed from static data. ^{129}Xe NMR data[48] highlighted Xe mobility in the channels, due to rapid intra-cage exchange. However, SS-NMR cannot locate Xe atoms in the channels and distinguish the thermal behaviors of different Xe sites, because, all the configurations of Xe inside the same cage are averaged in a single NMR feature.[48] On the one hand, this ADP variation makes the demodulated pattern noisier than the theoretical one from simulated data, and its refinement was not perfect. On the other hand these variation from ideality can give information on the mobility of Xe inside the channel. More information can be retrieved by solving the "inverse MED problem" as defined in ref. 16, the topic of a separate paper. Comparing the positions from static refinements (referring to a single temperature) and those from demodulated patterns (referring to all T range) can already give information of Xe mobility. In fact, the straight channel is aligned along [010], and the x and z coordinates of Xe atoms are always found correctly, because of their special position. Conversely their y coordinates can vary along the channel itself because of Xe disorder and the various MED experiment in Table 1 suggest different values along the channel. The sinusoidal channel is winding along [100] and now y is found correctly while x and z are only approximatively found, because of the Xe disorder along the channels, highlighting their mobility.

5. Conclusions

The MED theory[16] was at first probed by a simulated experiment (§3.3). This experiment allowed demonstrating that the 2Ω demodulated pattern contains the crystallographic information

coming selectively from the active species of the sample, i.e. the part of the sample responding to the stimulus. MED can therefore be defined as a "selective diffraction experiment". If the experimental conditions can be set up so that a chemical species only (an atom, a molecule, a substructure) responds selectively to the stimulus (as, in a first approximation Xe inside MFI channels) an unprecedented chemical selectivity in X-ray diffraction can be exploited to solve or analyze the substructure alone. By exploiting an increased sensitivity, the method we propose here is the adaptation of MES to diffraction, to exploit the possibility of filtering only the signal of the sample component responding to the stimulus. MED allowed obtaining the powder diffraction pattern of the active subset, i.e. obtaining selectively the crystallographic information on Xe by demodulation (i.e. mathematically treating the diffraction data by the PSD or PCA) of both simulated and experimental data. PCA and PSD resulted able to collect the first component (1Ω in PSD and PC1 in PCA) with very similar efficiency and precision. Conversely discrepancies between 2Ω and PC2 are observed, but they did not hamper the use of PC2 for substructure solution, because most of the error in PC2 loading resides in the 2 low angle peaks, that are not fundamental for the structure solution process. The 2Ω demodulated patterns were used to solve the crystal structure of the active species only, demonstrating the chemical selectivity of MED. The simulated MED experiment allowed obtaining the proof of principle of the theory and the real MED experiment allowed exploring the actual feasibility of the MED approach, and its potentialities and limitations.

The selectivity of PCA/PSD methods to Xe substructure was exploited to localize the Xe atoms. Also the dynamic of Xe atoms during adsorption and desorption was unravelled.

It is worth noting that the selectivity towards Xe is reached by exploiting neither its large atomic number, implying a large scattering power, nor the possibility of collecting resonant scattering data using X-ray diffraction measurements at the Xe adsorption edge. Therefore the proposed method can be applied also to light elements (also hydrogen in principle) and molecules, provided that the electron density of the light molecular moiety can be modulated by an external stimulus. In fact the experiment described in this paper can be considered as a "chemical modulation". It must be noticed that analysing the demodulated pattern, containing only the "virtual XRPD" of the adsorbed atom or molecule alone is much easier then refining its position in the standard XRPD pattern where its diffraction is hidden by the prevailing static framework information.[1-5]

Combining MED with PCA, an additional advantage is reached. In fact PCA does not require any pre-treatment and can be carried out "in real time" during data collection to check the quality of the data and modify and improve data collection, thus becoming an important tool for a successful application to MED data as a routine technique. This aspect is of paramount importance, taking into account the advent of modern detectors of the Pilatus series,[39] allowing routinely the collections of thousands of in situ XRPD dataset in 2-3 days of a synchrotron experiment. The PCA method proposed in the present paper can become a routine test method to assess the correctness of the experimental setup during *in situ* and *operando* experiments. Envisaging further applications of PSD/PCA applied to MED data, the simplest one could be in the indexation of the diffraction pattern of microporous samples also containing non porous crystalline impurities (a rather common case that is often resistant to standard indexation approaches). If the external stimulus is a gas pressure, clearly the microporous compound responds to the stimulus and its peak can be found and distinguished from the impurity peaks that are not modified by the stimulus, i.e. do not respond to the stimulus. Also peak extraction in powder diffraction can be improved, because different peaks respond differently to different stimuli and can be much more precisely identified than with standard Le Bail or Pawley methods, as implemented in the TOPAS software.[40,41] This method can be seen as an evolution of that proposed by Brunelli et al.[49] These results indicate that MED can become a very powerful tool in the analysis of materials and chemical compounds both as an innovative structure solution approach and as a way to analyze structure variations in operando conditions. Wide applications in the structure analysis of periodically changing materials (magnetic information storage systems, electrochemical systems such as batteries, solar cells etc.) may be envisaged for MED analysis. In addition, MED could also improve the efficiency of the current phasing methods. In fact, the time (t) variable may not only be introduced into the diffraction intensities, but also directly into crystallographic phasing procedures, such as Patterson, Fourier or direct methods. In this way PCA/PSD-improved difference Fourier syntheses, electron density and Patterson maps, filtered through their demodulation, could be envisaged, so that the sample response to the periodic stimulus is directly extracted from the diffraction patterns.

Acknowledgements: A. Urakawa (ICIQ, Tarragona, Spain) and W. van Beek and D. Chernyshov (SNBL, Grenoble, France) are acknowledged for their support and useful discussions during data collection and analysis and for PCA analysis by *The Unscrambler* software. L.P. acknowledges financial contributions by the MIUR project "Multidisciplinary modeling of the structure of layered materials" funded as FIRB in 2012, (code RBFR10CWDA) for funding his bursary.

Notes and references

[a] *Dipartimento di Scienze e Innovazione Tecnologica, Università del Piemonte Orientale ''A. Avogadro'' (Italy), Via Michel 11, I-15121 Alessandria, Italy. E-mail: marco.milanesio@uniupo.it*

[b] *Nova Res s.r.l., Via Dolores Bello 3, 28100 Novara, Italy (http://www.novares.org)*

[c] *Institute of Crystallography, CNR, via Amendola 122/o, Bari 70126, Italy.*

† Electronic Supplementary Information (ESI) available: Details of PSD theory, on simulated and experimental MED data by changing the stimulus amplitutred and related PSD/PCA analyses are reported. See DOI: 10.1039/b000000x/

1 G. Agostini, C. Lamberti, L. Palin, M. Milanesio, N. Danilina, B. Xu, M. Janousch, J. A. van Bokhoven, J. Am. Chem. Soc., 2010, 132 (2), 667-678

2 L. Palin, G. Croce, D. Viterbo, M. Milanesio, Chem. Mater., 2011, 23 (22) 4900–4909

3 M. Milanesio, G. Croce, D. Viterbo, H. O. Pastore, A. J. dos Santos Mascarenhas, E. C. de Oliveira Munsignatti, and L. Meda, A, J. Phys. Chem. A, 2008, 112 (36), 8403-8410.

4 M. Milanesio, C. Lamberti, R. Aiello, F. Testa, M. Piana, D. Viterbo, J. Phys. Chem. B., 104, 2000, 9951-9953.

5 L. Palin, C. Lamberti, Å Kvick, F. Testa F., R. Aiello, M. Milanesio, D. Viterbo, J. Phys. Chem. B., 2003, 107(17), 4034-4042.

6 J. L. Hodeau, V. Favre-Nicolin, S. Bos, H. Renevier, E. Lorenzo, J. F. Berar, Chem. Rev. 2001, 101, 1843-1867.

7 K. S. Wilson, Acta Crystallogr., 1978, B34, 1599–1608.

8 A. K.Mukherjee, J.R.Helliwell, P. Main, Acta Cryst. 1989. A45, 715-718.

9 G.M. Sheldrick, Acta Cryst., 2008, A64, 112-122.

10 M.C. Burla, R. Caliandro, M. Camalli, B. Carrozzini, G. L. Cascarano, L. De Caro, C. Giacovazzo, G. Polidori, D. Siliqi, R. Spagna, J. Appl. Cryst., 2007, 40, 609-613.

11 C. Giacovazzo, D. Siliqi, Acta Cryst. 2004, D60, 73-82.

12 D. Bourgeois, A. Royant, Curr Opin Struct Biol., 2005, 15(5), 538-547.

13 T.W. Kim, J. Hyuk Lee, J. Choi, K. Hwan Kim, L. J. van Wilderen, L. Guerin, Y. Kim, Y. Ouk Jung, C. Yang, J. Kim, M. Wulff, J.J. van Thor, H. Ihee, J. Am. Chem. Soc., 2012, 134 (6), 3145–3153.

14 J. Alex, M. Bader, M. Iten, D. Reimann, J. Troxler, U. Gensch, M. Grimberg, L. Jachmann, W. Koehler, H. Leich, M. Penno, R. Wenndorff. S. Choroba, H.-J. Eckoldt, T. Grevsmuehl, 2009, Proceedings of PAC09, Vancouver, BC, Canada.

15 Z. Ren, P. W. Y. Chan, K. Moffat, E. F. Pai, W. E. Royer Jr, V. Srajera X. Yang, Acta Cryst, 2013, D69, 946-959

16 D. Chernyshov, W. van Beek, H. Emeric h, M. Milanesio, A. Urakawa, D. Viterbo, L. Palin, R. Caliandro, Acta Cryst. 2011, A67 327-335.

17 D. Baurecht, U.P. Fringeli, Rev. Sci. Instrum. 2001, 72, 3282.

18 A. Urakawa, T. Bürgi, A. Baiker, J. Chemical Physics, 2006, 324, 653-658.

19 V. Marchionni, M. A. Newton, A. Kambolis, S. K. Matam, A. Weidenkaff, D. Ferri, Catalysis Today, 2014, 229, 80–87.

20 C. F. J. König, J. A. van Bokhoven, T. J. Schildhauer, M. Nachtegaal, J. Phys. Chem. C 2012, 116, 19857−19866.

21 J Stötzel, D Lützenkirchen-Hecht, R Frahm, J-D Grunwaldt, Journal of Physics: Conference Series, 2013, 430. 012126.

22 A. Urakawa, W. Van Beek, M. Monrabal-Capilla, J. R. Galàn-Mascaròs, L. Palin, M. Milanesio, J. Phys. Chem. C, 2011, 115, 1323.

23 W. van Beek, H. Emerich, A. Urakawa, L. Palin, M. Milanesio, R. Caliandro, D. Viterbo, D. Chernyshov, J. Appl. Cryst., 2012, 45, 738-747.

24 R. Caliandro, D. Chernyshov, H. Emerich, M. Milanesio, L. Palin, A. Urakawa, W. van Beek, D. Viterbo, J. Appl. Cryst., 2012, 45, 458-470.

25 D. Ferri, M. A. Newton, M Di Michiel, S. Yoon, G. L. Chiarello, V. Marchionni, S. K. Matam, M. H. A. A. Weidenkaff, F.i Wend, J. Gieshoffd, Phys. Chem. Chem. Phys., 2013, 15, 8629-8639

26 Y. Lu, S. Keav, V. Marchionni, G.L. Chiarello, A. Pappacena, M. Di Michiel, M. a. Newton, A. Weidenkaff, D. Ferri, Catal. Sci. Technol, 2014, 4, 2919-2031.

27 D. Ferri, M. A. Newton, M. Di Michiel, G. L. Chiarello, S. Yoon, Y. Lu, J. Andrieux, Angew. Chem., Int. E., 2014, 53(34), 8890–8894.

28 G. L. Chiarello, D. Ferri, Phys. Chem. Chem. Phys., 2015, DOI: 10.1039/C5CP00609K.

29 J. C. Burley, D. O'Hare, G. R. Williams, Anal.Methods , 2011, 3, 814-821.

30 H. Torigoe, K. Gotoh, T. Mori, H. Kobayashi, H. Ishida, K. Fujie, T. Ohkubo, H. Yamashita, Y. Kuroda, J. Phys. Chem. Lett. 2010, 1, 2642–2650.

31 X. Wang, S. Hu, W. Li, Q. Liu, S. Xiong, B. Chen, Q. Wang and Y. Tang, advanced article,, J. Mater. Chem. A, 2015, DOI: 10.1039/C5TA00460H..

32 I. Dmochowski, Nature Chem. 2009, 1, 250.

33 C. Sanloup, B.C. Schmidt, E.M.C. Perez, A. Jambon, E. Gregoryanz, M. Mezouar, M., Science, 2005, 310, 1174–1177.

34 V. Gianotti, G. Favaro, L. Bonandini, L. Palin, G. Croce, E. Boccaleri, E. Artuso, W. van Beek, C. Barolo, M., Chem. Sus. Chem., 2014, 7(11), 3039-3052.

35 G. Barr, W. Dong, C. J. Gilmore, J. Appl. Cryst. (2004). 37, 243-252

36 R. Caliandro, G. Di Profio, O. Nicolotti, J. Pharm. Biomed. Anal., 2013, 78/79, 269-279.

37 http://www.snbl.eu

38 W. van Beek, F. Carniato, S. Kumar, G. Croce, E. Boccaleri, M. Milanesio, Phase Trans., 2009, 82(4), 293-302.

39 P. Kraft, A. Bergamaschi, C. Broennimann, R. Dinapoli, E.F. Eikenberry, B. Henrich, I. Johnson, A. Mozzanica, C.M. Schleputz, P.R. Willmott, B. Schmitt, J. Synch. Rad.. 2009, 16, 368−375.

40 A.A. Coelho J. Appl. Cryst., 2003, 36, 86-95.

41 A.A. Coelho, J. Appl. Cryst., 2005, 38, 455-461.

42 MATLAB and Statistics Toolbox Release 2012b, The MathWorks, Inc., Natick, Massachusetts, United States

43 R. Caliandro, B. D. Belviso J. Appl. Cryst. 2014, 47, 1087-1096.

44 The Unscrambler, v10.2; CAMO Software Inc.: Woodbridge, NJ, 2012.

45 Agreement factor between PCA (I_{PCA}) and PSD (I_{PSD}) demodulated intensities was calculated as $R_{int} = |I_{PSD} - I_{PCA}|/|I_{PCA}|$

46 A. Altomare, C. Cuocci, C. Giacovazzo, A. Moliterni, R. Rizzi, N. Corriero and A. Falcicchio, J. Appl. Cryst., 2013. 46, 1231-1235.

47 IUCr general assembly, Montreal, abstract MS79O05

48 C. J. Jameson, A. K. Jameson, R. E. Gerald II, H.-M. Lim, J. Phys. Chem. B, 1997, 101(42), 8418.

49 M. Brunelli, J P. Wright, G.B.M. Vaughan, A. J. Mora, A. N. Fitch, Angew. Chem., Int. E., 2003, 115(18), 2075-2078.